Ca^{2+} influx and protein scaffolding via TRPC3 sustain PKCβ and ERK activation in B cells

Takuro Numaga[1,2], Motohiro Nishida[3], Shigeki Kiyonaka[1,4], Kenta Kato[1], Masahiro Katano[1], Emiko Mori[1], Tomohiro Kurosaki[5], Ryuji Inoue[6], Masaki Hikida[7], James W. Putney, Jr[2] and Yasuo Mori[1,4,*]

[1]Department of Synthetic Chemistry and Biological Chemistry, Graduate School of Engineering, Kyoto University, Kyoto 615-8510, Japan
[2]Laboratory of Signal Transduction, National Institute of Environmental Health Sciences, National Institutes of Health, Department of Health and Human Services, Research Triangle Park, NC 27709, USA
[3]Department of Pharmacology and Toxicology, Graduate School of Pharmaceutical Sciences, Kyushu University, Higashi-ku, Fukuoka 812-8582, Japan
[4]CREST, JST, Chiyoda-ku, Tokyo 102-0075, Japan
[5]Laboratory for Lymphocyte Differentiation, RIKEN Research Center for Allergy and Immunology, Tsurumi-ku, Yokohama, Kanagawa 230-0045, Japan
[6]Department of Physiology, School of Medicine, Fukuoka University, Jonan-ku, Fukuoka 814-0180, Japan
[7]Center for Innovation in Immunoregulative Technology and Therapeutics, Graduate School of Medicine, Kyoto University, Kyoto 606-8501, Japan
*Author for correspondence (mori@sbchem.kyoto-u.ac.jp)

Accepted 18 December 2009
Journal of Cell Science 123, 927-938

doi:10.1242/jcs.061051

Summary

Ca^{2+} signaling mediated by phospholipase C that produces inositol 1,4,5-trisphosphate [Ins(1,4,5)P_3] and diacylglycerol (DAG) controls lymphocyte activation. In contrast to store-operated Ca^{2+} entry activated by Ins(1,4,5)P_3-induced Ca^{2+} release from endoplasmic reticulum, the importance of DAG-activated Ca^{2+} entry remains elusive. Here, we describe the physiological role of DAG-activated Ca^{2+} entry channels in B-cell receptor (BCR) signaling. In avian DT40 B cells, deficiency of transient receptor potential TRPC3 at the plasma membrane (PM) impaired DAG-activated cation currents and, upon BCR stimulation, the sustained translocation to the PM of protein kinase Cβ (PKCβ) that activated extracellular signal-regulated kinase (ERK). Notably, TRPC3 showed direct association with PKCβ that maintained localization of PKCβ at the PM. Thus, TRPC3 functions as both a Ca^{2+}-permeable channel and a protein scaffold at the PM for downstream PKCβ activation in B cells.

Key words: B-cell receptor, Ca^{2+} signaling, Diacylglycerol, PKCβ, TRP channels

Introduction

Calcium signaling evoked by stimulation of plasma membrane (PM) receptors linked to phospholipase C (PLC) plays a central role in lymphocyte activation through production of inositol 1,4,5-trisphosphate [Ins(1,4,5)P_3] and diacylglycerol (DAG) (Berridge, 1993). In B cells, distinct patterns of Ca^{2+} signaling produced by B-cell receptor (BCR) engagement dictate alternative programs of transcription factor activation and thereby distinct cell fate (Liu et al., 2005). Ins(1,4,5)P_3 receptor mediates Ca^{2+} release from the internal Ca^{2+} stores of endoplasmic reticulum (ER). In addition, Ca^{2+} influx through diverse Ca^{2+}-permeable ion channels is activated by various triggers to control Ca^{2+} signaling (Fasolato et al., 1994). Among these are store-operated Ca^{2+} channels (SOCs, or capacitative Ca^{2+} entry channels), that are activated through Ins(1,4,5)P_3-induced Ca^{2+} release and consequent depletion of Ca^{2+} from ER stores (Putney, 1990). The physiological significance of Ca^{2+} influx via SOCs in lymphocytes has been extensively documented (Gallo et al., 2006). Electrophysiological analyses demonstrate that the Ca^{2+} release-activated Ca^{2+} (CRAC) channel is the SOC that initiates a Ca^{2+}-dependent signaling cascade via calcineurin and the transcription factor nuclear factor of activated T cells (NFAT) responsible for T cell activation (Lewis, 2001). Importantly, the T cells of patients with severe immunodeficiency display a specific defect in Ca^{2+} influx associated with the absence of CRAC channels (Partiseti et al., 1994). CRAC channels have also been reported in B cells, where they potentiate BCR-mediated Ca^{2+} signaling through Ca^{2+} oscillations and NFAT activation (Mori et al., 2002). However, it is known that in non-excitable cells, other Ca^{2+}-permeable channels may be activated directly by intracellular messengers such as DAG, Ca^{2+}, Ins(1,4,5)P_3 and arachidonic acid and its metabolites produced downstream of PLC (Fasolato et al., 1994; Bird et al., 2004; Parekh and Putney, 2005). Notably, B cells isolated from the above-mentioned patients with a defect in CRAC activity are capable of mounting normal immune responses (Partiseti et al., 1994; Le Deist et al., 1995; Feske et al., 2001), suggesting that Ca^{2+} influx pathways other than SOCs play essential roles in physiological responses of B cells.

Drosophila transient receptor potential (trp) protein (TRP), which was discovered through genetic studies of a *Drosophila* visual transduction mutation (Montell and Rubin, 1989), and the invertebrate and vertebrate TRP homologues of the so-called 'canonical' subfamily TRPC are channels that may mediate Ca^{2+} influx induced by activation of PLC-coupled receptors (Nishida et al., 2006). TRP homologues were originally hypothesized to encode SOCs, and some supportive evidence for this hypothesis was obtained from cDNA expression and gene knockout experiments for various TRP subtypes (Parekh and Putney, 2005). However, store-independent activation of Ca^{2+} influx and cation currents mediated by TRP channels seem to be the more common function of this channel family, especially the TRPCs (Hofmann et al., 2000; Bird et al., 2004; Parekh and Putney, 2005). Among the seven members of vertebrate TRPCs (TRPC1-7), TRPC2, TRPC3, TRPC6 and TRPC7 have been reported to be activated by DAG (Hofmann et al., 1999; Okada et al., 1999; Lucas et al., 2003). With regard to

the physiological importance of these DAG-activated cation channels (DACCs), previous studies have demonstrated their function as nonselective cation channels inducing membrane depolarization, which in turn activates voltage-dependent channels to induce action potentials (Lucas et al., 2003) and/or depolarization-induced Ca^{2+} influx, which is responsible for Ca^{2+}-dependent cellular responses such as muscle contraction (Inoue et al., 2001; Welsh et al., 2002) and activation of transcription factor NFAT (Thebault et al., 2006; Onohara et al., 2006). However, in contrast to the depolarizing function in excitable cells, the physiological significance of Ca^{2+} entry occurring directly through DACCs and subsequent Ca^{2+} signals is largely unknown.

DAG is recognized classically as the potent activator of protein kinase C (PKC), a family of serine/threonine kinases that play crucial roles in a plethora of biological functions, such as proliferation, differentiation, development and more specialized cellular functions (Nishizuka, 1995). The 'so-called' conventional PKCs (cPKCs) are activated by recruitment of the protein to membranes via the Ca^{2+}-dependent binding of C2 domains to phospholipids, which is potentiated by the binding of C1 domains to DAG. Spatial and temporal targeting critical for the enzymatic activation of cPKC is mostly driven by the spatial and temporal properties of the Ca^{2+} signaling machinery (Oancea and Meyer, 1998; Maasch et al., 2000; Pinton et al., 2002; Mogami et al., 2003; Reither et al., 2006). Specifically, local changes in intracellular Ca^{2+} concentration ($[Ca^{2+}]_i$) control membrane translocation of cPKCs, and different modes of Ca^{2+} influx and release target cPKCs to distinct areas in the cell (Maasch et al., 2000; Pinton et al., 2002). In B cells, PKCβ isoforms are the major Ca^{2+} and DAG-regulated cPKCs (Mischak et al., 1991), and their important roles in BCR signaling and cell survival have been demonstrated using PKCβ-knockout mice with impaired humoral immune responses and reduced cellular responses of B cells (Leitges et al., 1996). However, despite the physiological importance of PKCβ established in the context of B-cell biology, specific subtypes of Ca^{2+}-permeable channels responsible for PKCβ translocation and activation have not been elucidated in B cells.

Previous studies have suggested that activation of PKCβ and the duration of activation of a mitogen-activated protein (MAP) kinase, extracellular signal-regulated kinase (ERK), play important roles in development of B cells (King and Monroe, 2000; Koncz et al., 2002). Immature B cells undergo apoptosis upon BCR stimulation to eliminate self-antigen reactive cells, whereas mature B cells proliferate and differentiate by BCR stimulation. It has been demonstrated that this differential functional response of immature and mature B cells is partly attributable to the activation of PKCβ and differences in the duration of ERK activation. In immature B cells, ligation of BCR is uncoupled from the activation of PKCβ (King and Monroe, 2000), and transient phosphorylation of ERK and activation of ERK-dependent transcription factors are involved in triggering apoptosis. In mature B cells, sustained ERK activation induces survival and cell activation (Koncz et al., 2002). Furthermore, we previously demonstrated that Ca^{2+} entry is coupled to translocation and secondary activation of PLCγ2, which amplifies Ins(1,4,5)P_3 production and Ca^{2+} signaling upon BCR stimulation in the avian B cell line DT40 (Nishida et al., 2003). The same Ca^{2+} entry mechanism also induced sustained MAP kinase signaling that was sensitive to blockade by PKC inhibitors. This, together with the above-stated importance of temporal patterns in controlling BCR responses, has prompted us to now investigate the Ca^{2+} entry mechanism linked to DAG and PKC signaling at the 'sustained' phase.

Here, we describe an investigation of DACCs and their physiological significance in the context of BCR signaling. In DT40 cells, genetic disruption of translocation of TRPC3 proteins to the PM has revealed that native TRPC3 forms DACCs but not SOCs. Upon BCR activation, the DAG-activated Ca^{2+} influx via TRPC3 amplifies Ca^{2+} signals and downstream NFAT activation by controlling PM translocation of PLCγ2 and sustains PKCβ translocation and activation. Furthermore, direct physical interaction between TRPC3 and PKCβ also regulates the stable retention of PKCβ at the PM, leading to the sustained BCR-induced MAP kinase activation. These results suggest that TRPC3 has a dual function in BCR-induced signaling: it is a DACC, which elicits PM translocation of PLCγ2 and PKCβ, and a scaffolding platform at the PM for PKCβ.

Results

Disruption of PM expression of endogenous TRPC3 channels in DT40 B cells

The expression of DAG-activated TRPC3 and TRPC7 channels was previously demonstrated in DT40 cells (Nishida et al., 2003). Furthermore, recombinant expression studies suggested that TRPC3 channels are in part responsible for Ca^{2+} entry associated with translocation and sustained activation of PLCγ2 (Nishida et al., 2003). Therefore, to study the possible physiological significance of DAG-activated Ca^{2+}-permeable TRPC3 channels in PLCγ2-mediated BCR signaling, the *TRPC3* gene locus was disrupted by deletion of the exon encoding amino acid residues (a.a.) 681-750, containing the well conserved TRP domain (Okada et al., 1999), through homologous recombination in DT40 B cells (Fig. 1A,B). RT-PCR revealed that TRPC3-mutant (MUT) DT40 cells expressed truncated TRPC3 transcripts in which the targeted exon was deleted (Fig. 1C), in accordance with immunoblotting detecting a slightly smaller band in MUT cells (Fig. 1D). Evaluation of channel function of mouse TRPC3 (mC3) with the corresponding deletion [mC3(Δ667-736): a.a. 667-736 in mC3 corresponds to a.a. 681-750 in chicken TRPC3] revealed that it lacks Ca^{2+} influx channel activity upon stimulation by ATP, carbachol (CCh), and the membrane permeable DAG analogue, 1-oleolyl-2-acetyl-*sn*-glycerol (OAG), when expressed in the HEK293 cell system (supplementary material Fig. S1A). Confocal images revealed an intracellular localization of a mC3(Δ667-736)-EGFP fusion construct, in contrast to WT mC3-EGFP which was localized in the PM (supplementary material Fig. S1B). These results clearly indicate that deletion of the TRP domain ablates targeting of TRPC3 proteins to the PM. Consistent with these results, immunofluorescence staining using anti-TRPC3 antibody revealed intracellular localization of TRPC3 proteins in MUT cells but PM localization in WT cells, suggesting that the endogenous truncated mutant of TRPC3 in MUT cells has a defect in PM expression (supplementary material Fig. S1C). The level of cell surface expression of BCR examined by staining with FITC-conjugated anti-chicken IgM antibody on MUT clones was indistinguishable from that of parental DT40 cells (supplementary material Fig. S1D).

TRPC3 constitutes a DACC but not SOC in DT40 B cells

DAG-induced ionic currents in WT and MUT DT40 cells were analyzed using the whole-cell patch-clamp technique (Fig. 1E-G). In WT cells, bath application of 10 μM OAG induced relatively sustained inward currents (1.74±0.45 pA/pF, n=7) at a holding potential of –60 mV (Fig. 1G). The current-voltage (*I-V*) relationship showed a slight outward rectification similar to the recombinant

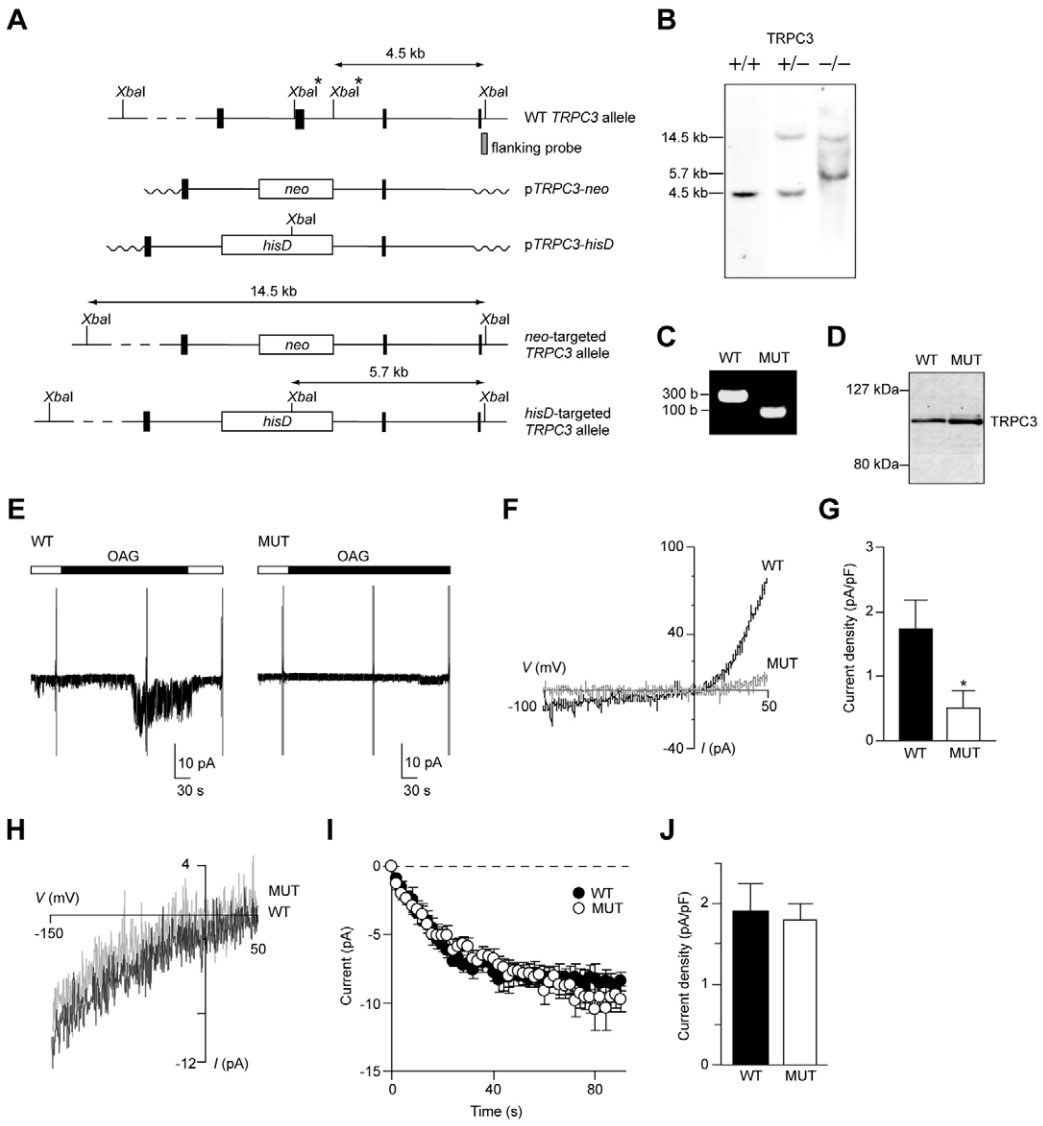

Fig. 1. TRPC3 forms a DACC in B cells. (**A**) Partial restriction map of the chicken *TRPC3* allele, targeting constructs and expected structure of the disrupted alleles. (**B**) Southern blot analysis of genomic DNAs from WT (+/+), *neo*-targeted (+/–), and *neo*/*hisD*-targeted (–/–) clones. (**C**) RT-PCR analysis of TRPC3 transcript expression in WT and MUT cells. (**D**) Immunoblotting of TRPC3 from WT and MUT cells. (**E**) Actual records at a holding potential of –60 mV in WT (left) and MUT cells (right) stimulated with 10 μM OAG. (**F**) *I-V* relationships of the 10 μM OAG-induced inward current obtained by subtracting currents before activation of channels from those after activation. (**G**) Peak OAG-induced current densities at –60 mV in WT (n=7) and MUT cells (n=8). *P<0.05, versus WT cells. (**H**) Representative leak-subtracted *I-V* relationships of I_{CRAC} evoked by 10 μM Ins(1,4,5)P_3 in WT (black) and MUT (grey) cells. Currents are evoked by 50-ms voltage-ramps from –150 to 50 mV. (**I**) Average time courses of I_{CRAC} at –130 mV in WT (n=4) and MUT cells (n=15). $[Ca^{2+}]_i$ was clamped to near 0 with 10 mM EGTA. The whole-cell configuration of the patch-clamp recording was established at the time 0. (**J**) Average current densities from the data in I at 80 seconds in WT (n=4) and MUT cells (n=15).

TRPC3 current (Lintschinger et al., 2000) with reversal potential of 0 mV (Fig. 1F). The time between OAG challenge and current activation varied among WT cells: the time to maximum current amplitude after OAG application was from 78 to 301 seconds and the average time to maximum was 196±31 seconds. In contrast to WT cells, MUT cells showed significantly reduced OAG-induced currents (0.51±0.27 pA/pF, n=8; Fig. 1E-G). BCR ligation induced rapid release of Ca^{2+} from internal stores and depletion of Ca^{2+} stores subsequently activating store-operated Ca^{2+} entry (SOCE), a major Ca^{2+} entry pathway in B cells (Mori et al., 2002). We compared Ca^{2+} release-activated Ca^{2+} currents (I_{CRAC}) that correspond to SOCE in WT and MUT cells. Intracellular dialysis with 10 μM Ins(1,4,5)P_3 via the patch pipette elicited inward currents that showed the salient features of I_{CRAC}: a positive reversal potential and inward rectification over the voltage range from –150 to 50 mV (Fig. 1H). Peak current densities and activation kinetics of I_{CRAC} recorded in MUT cells were comparable to those in WT cells (Fig. 1I,J). In $[Ca^{2+}]_i$ measurements, in the absence of extracellular Ca^{2+}, ionomycin, which fully depletes intracellular Ca^{2+} stores, caused a transient Ca^{2+} rise in both WT and MUT cells, indicating that stores are not affected by loss of TRPC3. Readmission of extracellular Ca^{2+} led to a comparable $[Ca^{2+}]_i$ increases in both WT and MUT cells (supplementary material Fig. S2). These results clearly indicate that DACCs are ablated, but SOCs are unaffected by the expression defect of functional TRPC3 channels at the PM in DT40 B cells.

TRPC3 plays a critical role in BCR-induced Ca^{2+} signaling in DT40 B cells

We next analyzed $[Ca^{2+}]_i$ mobilization in response to physiological stimuli via BCR in WT and MUT DT40 cells (Fig. 2). In the presence of 2 mM extracellular Ca^{2+}, $[Ca^{2+}]_i$ increases, induced by BCR ligation, were significantly suppressed in MUT cells (Fig. 2A,C). BCR-induced Ca^{2+} mobilization in MUT cells was indistinguishable from that in WT cells in the absence of extracellular Ca^{2+} (Fig. 2B,C), indicating that the Ca^{2+} response defect in MUT cells is attributable to Ca^{2+} influx defect. In support of this observation, the compromised Ca^{2+} influx in MUT cells was restored in MUT cells stably transfected with mC3 cDNA (Fig. 2A-C). The stable MUT transfectant exhibited immunolocalization of TRPC3 at the PM and intracellular TRPC3, which may represent exogenous mC3 and an endogenous TRPC3 truncation mutant, respectively (supplementary material Fig. S1C;

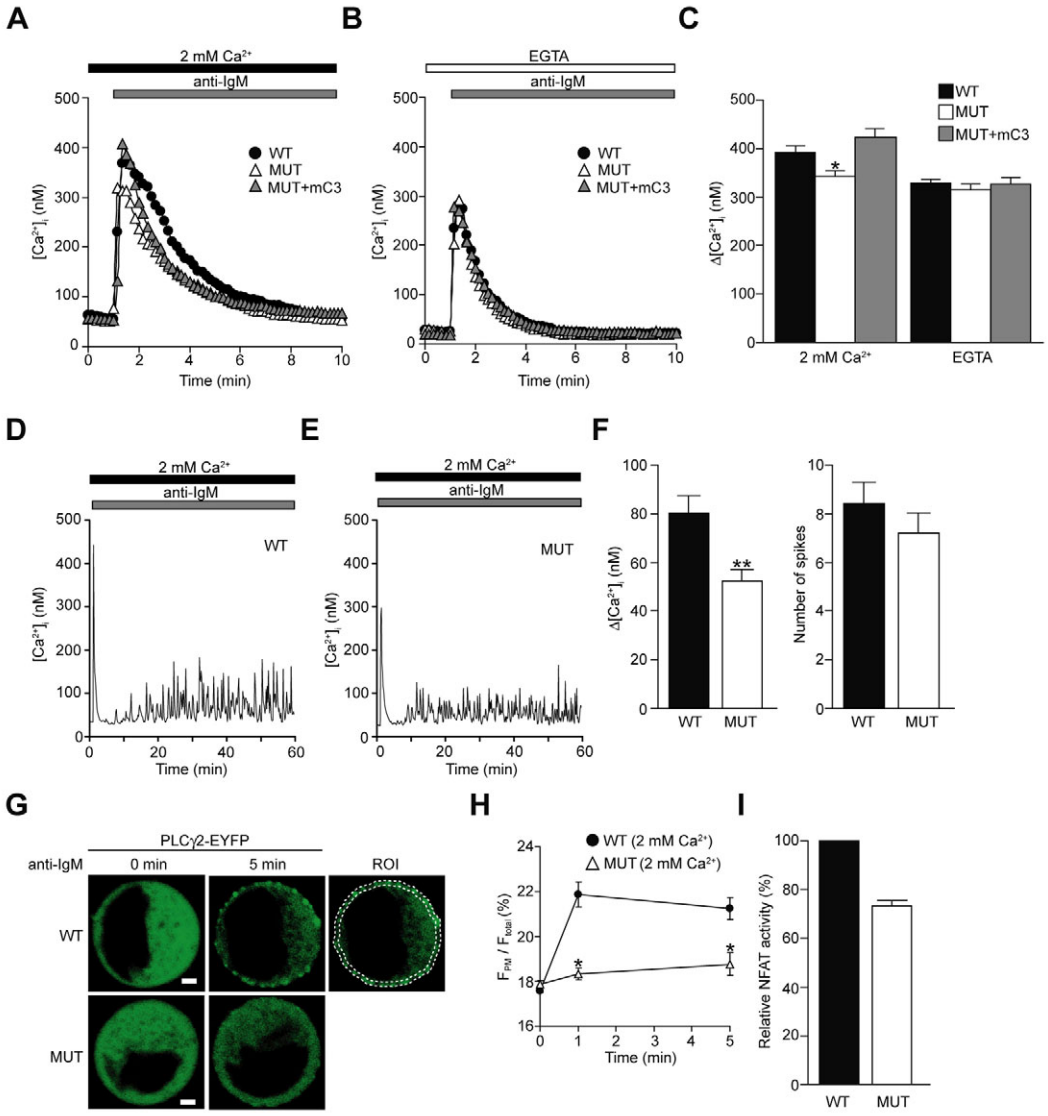

Fig. 2. TRPC3 contributes to BCR-induced Ca^{2+} mobilization and subsequent activation of NFAT. (**A**,**B**) Average time courses of Ca^{2+} responses evoked in the presence (A) or absence (B) of extracellular Ca^{2+} upon BCR stimulation with anti-BCR antibody (anti-IgM; 1 μg/ml) in WT (*n*=76-90), MUT (*n*=81-84) and MUT cells expressing recombinant mC3 (*n*=85-89). (**C**) Peak BCR-induced $[Ca^{2+}]_i$ rises in WT and MUT cells. **P*<0.05, versus WT cells. (**D**,**E**) Representative long time courses of BCR-induced Ca^{2+} responses in WT (D) and MUT (E) cells stimulated with 1 μg/ml anti-IgM in Ca^{2+}-containing solution (60 minutes). (**F**) Average of the peak $[Ca^{2+}]_i$ increases in oscillations (left) and average number of spikes (right) in WT (*n*=35) and MUT cells (*n*=32). Peak $[Ca^{2+}]_i$ rises were analyzed after 30 minutes of BCR stimulation. The number of spikes per 10 minutes after 30 minutes of BCR stimulation was counted. ***P*<0.01, versus WT cells. (**G**) Confocal images showing BCR-induced changes in the subcellular localization of PLCγ2-EYFP in WT and MUT cells stimulated with anti-IgM in Ca^{2+}-containing solution. Scale bars: 2 μm. Right panel shows ROI (between the two dashed lines) for quantification of fluorescent changes of PLCγ2-EYFP distributed in the area of the PM. A 0.5 μm width of the peripheral region was defined as the PM region. The area surrounded by the outer line was used to measure the total fluorescence (F_{total}). (**H**) Average time courses of fluorescent changes of PLCγ2-EYFP distributed in the PM area in WT (*n*=3) and MUT cells (*n*=3). **P*<0.05, versus WT cells. (I) NFAT activity in WT and MUT cells. Cells were stimulated with 10 μg/ml anti-IgM. NFAT activity of MUT cells relative to that of WT cells is shown.

Fig. S3A). The level of TRPC3 expression was nearly doubled in the stable MUT transfectant compared with the original MUT cells (supplementary material Fig. S3B). Thus, disruption of functional TRPC3 expression at the PM, which mediates DAG-activated currents, elicits a Ca^{2+} influx defect in DT40 B cells.

We have previously shown that BCR stimulation induces the initial Ca^{2+} responses followed by Ca^{2+}-entry-dependent sustained and/or oscillatory responses (Nishida et al., 2003). In MUT cells, the amplitudes of Ca^{2+} oscillations were reduced compared with those in WT cells (Fig. 2D-F) when the same concentration of anti-IgM (1 μg/ml) as Fig. 2A-C was employed for BCR stimulation. By contrast, the frequency of Ca^{2+} oscillation was indistinguishable between WT and MUT cells. This suggests that Ca^{2+} influx via DAG-activated TRPC3 channels is crucial for the modulation of Ca^{2+} oscillations.

A previous study revealed that Ca^{2+}-influx-dependent membrane translocation, secondary activation of PLCγ2 and secondary production of Ins(1,4,5)P_3 are required for the generation of Ca^{2+}

oscillations (Nishida et al., 2003). TRPC3 has been considered as a candidate for the unidentified molecular entity of that Ca^{2+} entry pathway, based on the observation that PLCγ2 was shown to be functionally and physically coupled to TRPC3 in a HEK293 heterologous expression system (Nishida et al., 2003). Thus, we next examined coupling of native TRPC3 channels with PLCγ2 translocation in DT40 cells by observing EYFP-tagged PLCγ2 (PLCγ2-EYFP) with time-lapse confocal laser microscopy. BCR ligation induced PM translocation of PLCγ2-EYFP in WT cells, whereas this was nearly abolished in MUT cells (Fig. 2G,H). Thus, the suppression of BCR-induced Ca^{2+} oscillations in MUT cells may be attributable to the defect in BCR-induced PLCγ2 translocation.

For PM translocation of PLCγ2, Ca^{2+} influx through TRPC3 is particularly important, because expression of red fluorescent protein (mStrawberry)-tagged mC3 (mC3-mStrawberry), but not that of mStrawberry-tagged mutant mC3 with a defect in the pore-forming region (mC3PD-mStrawberry), restored BCR-induced PLCγ2 translocation in MUT cells (supplementary material Fig. S4A). In addition, $[Ca^{2+}]_i$ elevation by ionomycin also failed to translocate PLCγ2 to the PM (supplementary material Fig. S4B). Interestingly, overexpression of an mStrawberry-tagged mC3 subfragment containing a.a. 23-73 [mStrawberry-mC3(23-73)], which interacts with PLCγ (van Rossum et al., 2005) and suppressed PLCγ2 translocation in WT cells, failed to recover the translocation defect of PLCγ2 in MUT cells (supplementary material Fig. S4C,D). This excludes the possibility that the PLCγ2 translocation defect in MUT cells endogenously expressing the truncated mutant TRPC3 is solely attributable to its dominant-negative effect anticipated from the co-immunoprecipitation of PLCγ2 with the counterpart mC3(Δ667-736) mutant in HEK293 cells (supplementary material Fig. S4E), and supports the importance of functional TRPC3 localized at the PM.

Downstream of Ca^{2+} oscillations, a Ca^{2+}-dependent transcription factor NFAT is activated to play a crucial role in lymphocyte activation (Rao et al., 1997; Peng et al., 2001). In addition, BCR stimulation activates NFAT through the BCR-induced PLC-Ca^{2+} signaling pathway (Sugawara et al., 1997). Interestingly, MUT cells showed an approximately 30% reduction in BCR-mediated NFAT activation compared with WT cells (Fig. 2I).

TRPC3-mediated Ca^{2+} influx is required for PM translocation of PKCβ

The secondary PLCγ2 activation should enhance production of DAG as well as Ins(1,4,5)P_3, since equimolar DAG and Ins(1,4,5)P_3 are generated through phosphatidylinositol 4,5-bisphosphate [PtdIns(4,5)P_2] hydrolysis by PLC. Therefore, we next examined the impact of TRPC3 deficiency on BCR-induced DAG production and its downstream PKC activation (Fig. 3). Among nine PKC subtypes, our study focused on cPKCs, particularly PKCβ isoforms, as potential target molecules of Ca^{2+} influx via TRPC3 channels, because of the requirement of Ca^{2+} and DAG for their activation as well as the fact that PKCβ isoforms are the major PKC isozymes expressed in B cells (Mischak et al., 1991). PM translocation of endogenous PKCβ was assessed using the membrane fractionation method, since PM translocation of PKC has been considered as the most critical step in its activation and has been frequently used to assess PKC activation (Liu et al., 1998). BCR stimulation caused sustained membrane translocation of PKCβ for at least 30 minutes in the presence of extracellular Ca^{2+} in WT cells (Fig. 3A). As observed for WT cells in the absence of extracellular Ca^{2+}, MUT cells exhibited transient PKCβ PM translocation in the presence of extracellular Ca^{2+}. The translocation defect was rescued by the recombinant expression of mC3 (Fig. 3A). Levels of BCR-dependent PKCβ activation were compared between WT and MUT cells by analyzing PM translocation of the EGFP fusion protein for PKCβII (PKCβII-EGFP), the most abundant PKCβ isoform in DT40 cells (T. N., unpublished data), at the single cell level using confocal microscopy. PKCβII-EGFP was diffusively distributed throughout the cytosol in resting cells, and rapidly translocated, within 1 minute, from cytosol to the PM upon BCR stimulation. In WT cells, PKCβII-EGFP translocation persisted in the presence of extracellular Ca^{2+} but became transient in the absence of extracellular Ca^{2+} (Fig. 3B,D). By contrast, in the presence of extracellular Ca^{2+}, PKCβII-EGFP translocation was transient in MUT cells. Although BCR-induced sustained translocation of PKCβII-EGFP to the PM was recovered by the expression of mC3-mStrawberry, mC3PD-mStrawberry failed to restore the defect in sustained PKCβII PM translocation in response to BCR stimulation in MUT cells (Fig. 3C,D). These studies suggest that TRPC3-mediated Ca^{2+} entry is required for BCR-induced PKCβII PM translocation.

Since translocation of PKCβ is affected by DAG via the C1 domain (Oancea and Meyer, 1998), we next analyzed the OAG-induced PM translocation of PKCβII-EGFP. Application of OAG to WT cells caused a clear translocation of PKCβII-EGFP to the PM in the presence of extracellular Ca^{2+}, whereas in the absence of extracellular Ca^{2+}, the OAG-induced translocation was nearly abolished (Fig. 3E,G). Interestingly, in the presence of extracellular Ca^{2+}, OAG failed to translocate PKCβII-EGFP to the PM in MUT cells. Although OAG-induced sustained translocation of PKCβII-EGFP to the PM was recovered by the expression of mC3-mStrawberry, mC3PD-mStrawberry again failed to restore the defect in sustained PKCβII PM translocation in response to OAG stimulation in MUT cells (Fig. 3F,G). These results suggest that OAG-activated Ca^{2+} influx mediated by TRPC3 is required for the OAG-induced PM translocation of PKCβII.

PKCβ carries the C2 domain that interacts with Ca^{2+} and anionic phospholipids, and cPKC is known to translocate to the PM in response to a rapid, generalized increase in $[Ca^{2+}]_i$ induced by ionomycin (Maasch et al., 2000) through passive leakage from Ca^{2+} stores and Ca^{2+} influx (supplementary material Fig. S2A). In fact, ionomycin evoked the accumulation of PKCβII-EGFP at the PM, which persisted for 10 minutes in WT cells. By contrast, PKCβII-EGFP failed to show significant accumulation at the PM in MUT cells (see data in the presence of U73343, an inactive analogue for the PLC inhibitor U73122 in supplementary material Fig. S5A). These results suggest that TRPC3 mediates localization of PKCβ at the PM induced by a generalized $[Ca^{2+}]_i$ increase. Interestingly, after PKCβII-EGFP transiently accumulated at the PM, it showed cytosolic localization at 10 minutes in WT cells pretreated with the PLC inhibitor U73122 (supplementary material Fig. S5A). Thus, activation of PLCγ2, production of DAG, and Ca^{2+} influx via DAG-activated TRPC3 channels may be involved in PM translocation of PKCβII-EGFP in response to a generalized $[Ca^{2+}]_i$ increase.

TRPC3 functions as a scaffold for BCR-induced sustained translocation of PKCβ to the PM in DT40 B cells

We next tested the possibility that PKCβ might colocalize with TRPC3 at the PM, given PM translocation of PKCβ upon BCR stimulation. PKCβ was co-immunoprecipitated with TRPC3 before BCR stimulation in the presence or absence of extracellular Ca^{2+} in WT and MUT DT40 cells (Fig. 4A). The association between

TRPC3 and PKCβ increased after 15 minutes BCR stimulation in an extracellular-Ca^{2+}-dependent manner in WT cells. By contrast, no such increase of interaction was observed after 15 minutes BCR stimulation in MUT cells. Interestingly, the increased phase of the interaction between TRPC3 and PKCβ coincided with the sustained phase of PKCβ PM translocation in which TRPC3 plays a critical role (Fig. 3A,B,D). We next assessed in vitro binding of the mC3 constructs with PKCβ in DT40 cell extracts or with the PKCβ

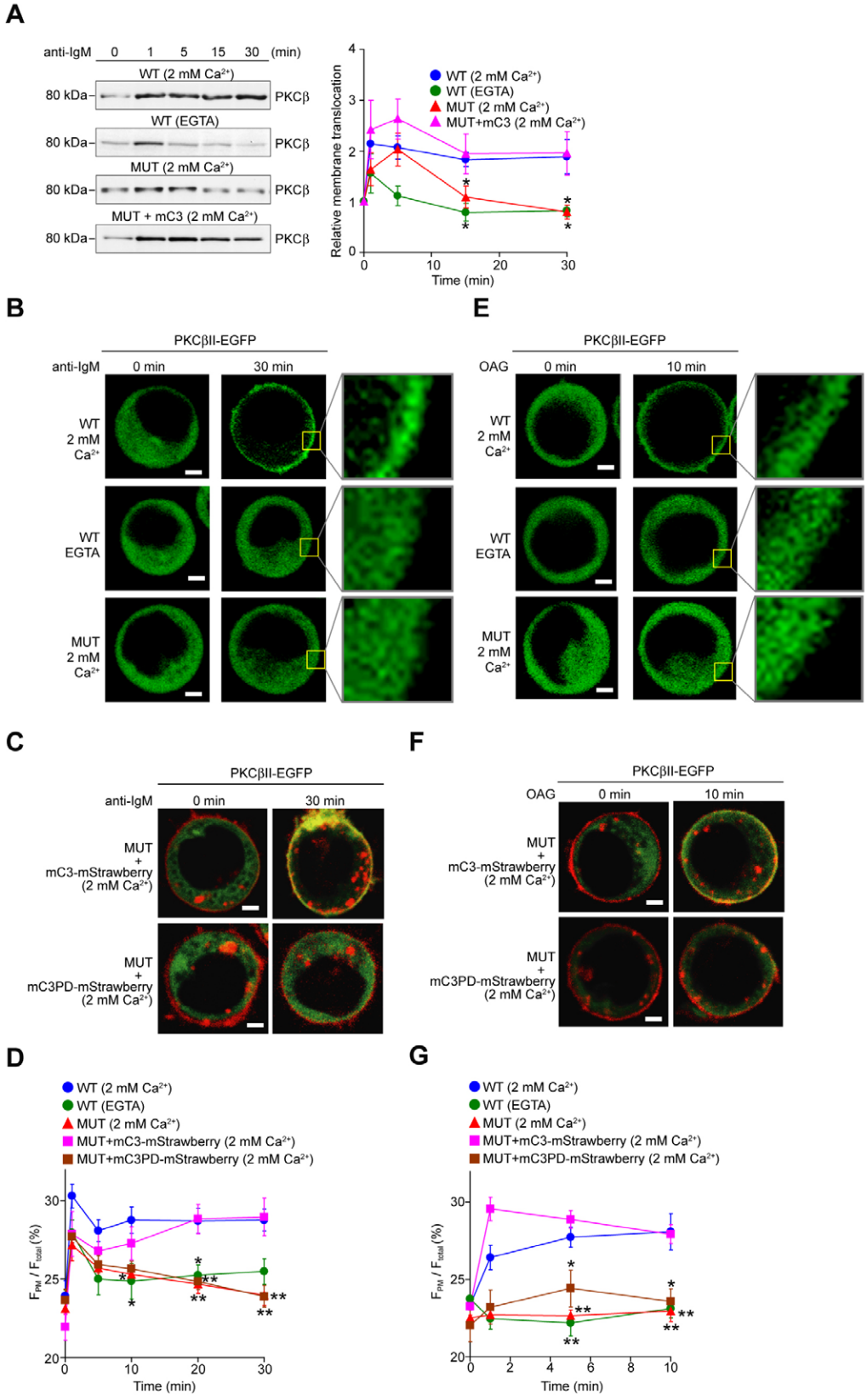

Fig. 3. TRPC3 maintains BCR-induced translocation of PKCβ to the PM in B cells. (**A**) BCR-induced membrane localization of endogenous PKCβ in WT and MUT cells. The graph depicts time courses of PKCβ membrane translocation relative to that in unstimulated cells. The membrane-bound PKCβ was analyzed by membrane fractionation and subsequent immunoblotting using PKCβ-specific antibody. (**B**) Confocal images of BCR-induced membrane translocation of PKCβII-EGFP in WT and MUT cells. Scale bars: 2 μm. Enlargements of the boxed regions are also shown in right panels. (**C**) Confocal images of BCR-induced membrane translocation of PKCβII-EGFP in MUT cells, expressing mC3-mStrawberry or mC3PD-mStrawberry. Scale bars: 2 μm. (**D**) The time courses of average BCR-induced changes in PKCβII-EGFP fluorescence distribution in PM regions in WT cells stimulated in the presence (n=11) or the absence (n=7) of extracellular Ca^{2+}, in MUT cells stimulated in the presence of extracellular Ca^{2+} (n=8), and in MUT cells expressing mC3-mStrawberry (n=7) or mC3PD-mStrawberry (n=7) stimulated in the presence of extracellular Ca^{2+}. (**E-G**) Confocal analyses of OAG-induced changes of subcellular localization of PKCβII-EGFP in WT and MUT cells. The sets of experiments performed in E, F and G are the same as those in B, C and D, respectively, except for the use of OAG for stimulation. In G, nine or five WT cells were analyzed in the presence or the absence of extracellular Ca^{2+}, respectively, while five MUT cells and six MUT cells expressing mC3-mStrawberry or mC3PD-mStrawberry were analyzed. ROI are defined in Fig. 2G. *P<0.05; **P<0.01, versus WT cells in the presence of extracellular Ca^{2+}.

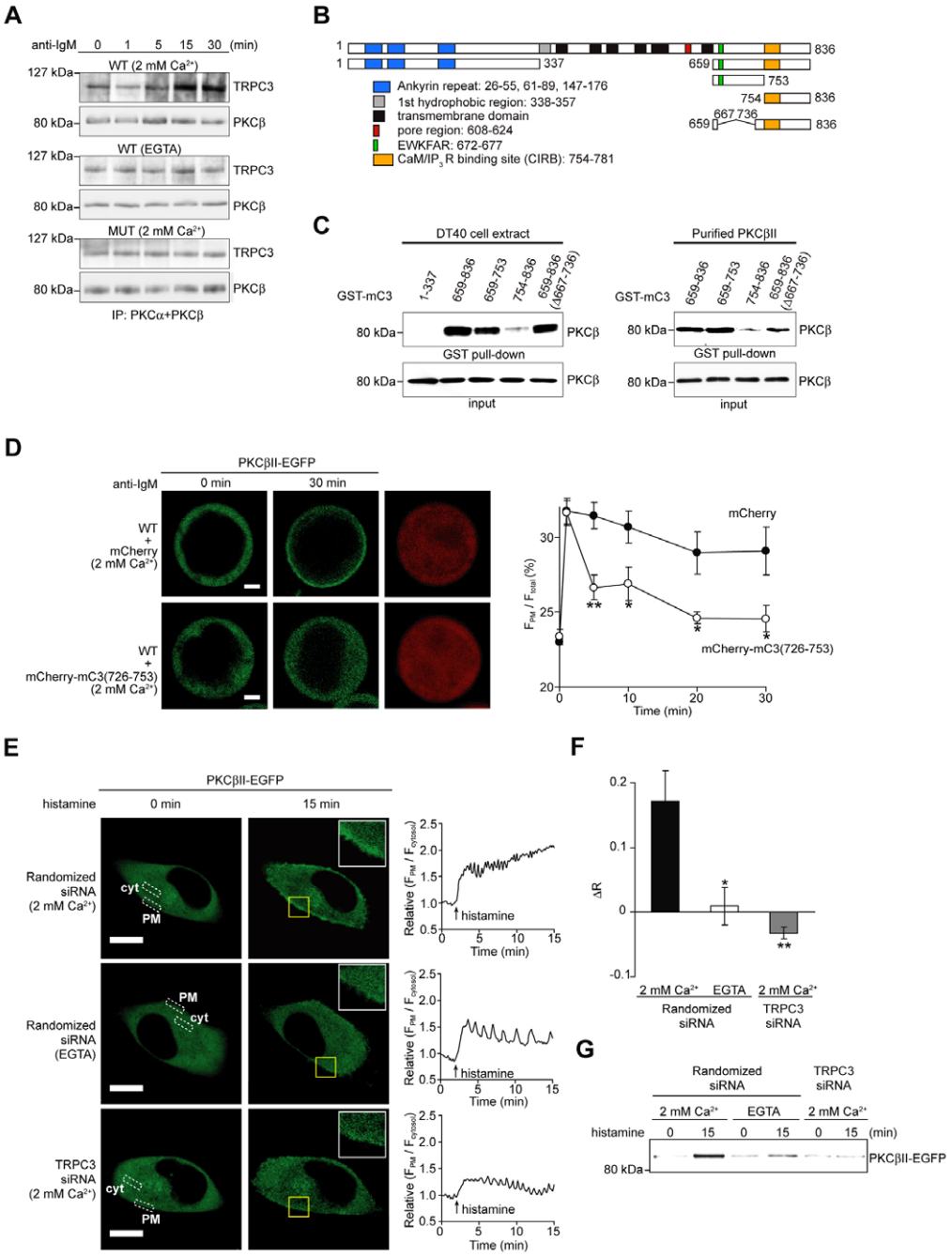

Fig. 4. Direct association of PKCβ with TRPC3. (**A**) Temporal changes of the complex formed between PKCβ and TRPC3. Within each pair of blots, upper and lower panel show co-immunoprecipitated TRPC3 and immunoprecipitated PKCβ, respectively. (**B**) A schematic representation of GST fusion mC3 subfragments. (**C**) Pull-down assay of PKCβ using GST fusion mC3 subfragments. DT40 cell extracts (left panels) or purified PKCβ preparations (right panels) were incubated with GST fusion mC3 subfragments immobilized on glutathione-Sepharose beads. Bound proteins were analyzed by immunoblotting using anti-PKCβ antibody. Inputs of each sample are shown in the lower panels. (**D**) Confocal images indicating BCR-induced membrane translocation of PKCβII-EGFP in WT DT40 cells expressing mCherry or mCherry-mC3(726-753). Subcellular distribution of mCherry and mCherry-mC3(726-753) are also shown. Scale bars: 2 µm. The graph represents the time courses of average changes in fluorescence of PKCβII-EGFP distributed in the PM regions in WT cells expressing mCherry (n=5) or mCherry-mC3(726-753) (n=5). ROI are defined in Fig. 2G. *P<0.05; **P<0.01, versus WT cells expressing mCherry. (**E-G**) The role of TRPC3 in translocation of PKCβ to the PM in HeLa cells. (E) Confocal images indicating histamine-induced membrane translocation of PKCβII-EGFP in HeLa cells transfected with TRPC3 siRNAs. Scale bars: 10 µm. The insets show enlarged views of the boxed regions. The traces on right show representative time courses of translocation of PKCβII-EGFP to the PM, given as the ratio (relative to time 0) of fluorescence intensity at the PM (F_{PM}) to that in the cytosol ($F_{cytosol}$). ROI on the PM and in the cytosol (cyt) are indicated in the 0 minute panels. The data are representative of five independent experiments. (F) TRPC3 siRNAs disrupt sustained association of PKCβII-EGFP with the PM 15 minutes after histamine stimulation. The changes of PM fluorescence intensity are expressed as ΔR (see Materials and Methods). Images obtained from the experiment performed in E were subjected to analysis. *P<0.05; **P<0.01, versus randomized siRNA-transfected cells stimulated in the presence of extracellular Ca^{2+}. (G) Histamine-induced membrane accumulation of PKCβII-EGFP in HeLa cells co-transfected with TRPC3 siRNAs. Cells were treated for 15 minutes with 100 µM histamine in the presence or absence of extracellular Ca^{2+}. The experiments were performed as in Fig. 3A.

purified preparations in a glutathione S-transferase (GST) pull-down assay (Fig. 4B,C). The TRPC3 C-terminal residues Asn659-Glu836 and Asn659-Phe753 bound to PKCβ, whereas residues of Asn754-Glu836 only showed faint interaction. Furthermore, deletion of Asp667-Arg736 at the C-terminus, which corresponds to deletion of the TRPC3 mutant expressed in MUT cells, failed to affect the interaction of TRPC3 with PKCβ in vitro (Fig. 4B,C). These results suggest that Asn659-Glu666 and/or Leu737-Phe753 (supplementary material Fig. S5B) are essential for the interaction of TRPC3 with PKCβ.

To investigate the functional relevance of the direct interaction between TRPC3 and PKCβ in PKCβ translocation, the effects of the transiently expressed PKCβ-interacting mC3 fragment (Leu726-Phe753) fused to red fluorescent protein mCherry [mCherry-mC3(726-753)] were tested on BCR-induced translocation of PKCβII-EGFP towards the PM in WT DT40 cells. mCherry alone and mCherry-mC3(726-753) were indistinguishable in their subcellular localization in WT cells (Fig. 4D). However, expression of mCherry-mC3(726-753) significantly suppressed the sustained phase of the BCR-induced PKCβ translocation compared with mCherry alone (Fig. 4D). Thus, TRPC3 residues Leu726-Phe753 are sufficient for disruption of PKCβ translocation to the PM, suggesting that TRPC3 is important in anchoring PKCβ to the PM through physical interaction as well as through eliciting Ca^{2+} influx.

TRPC3 is required for sustained localization of PKCβ at the PM in HeLa cells

PM translocation and activation of PKCβII have been previously analyzed using real-time imaging in HeLa cells (Violin et al., 2003). To examine the precise spatiotemporal patterns of the functional coupling between TRPC3 and PKCβ, we analyzed histamine-induced PM translocation of PKCβII-EGFP in HeLa cells using confocal microscopy. HeLa cells were transfected with small interfering RNAs (siRNAs) specific for human TRPC3 to knockdown endogenous TRPC3 levels (supplementary material Fig. S6). Histamine at a concentration of 100 μM evoked gradual concentration of the PKCβII-EGFP fluorescence at the PM after rapid accumulation in the initial phase, and the PM concentration of PKCβII-EGFP showed oscillations in control HeLa cells (Fig. 4E,F). The removal of extracellular Ca^{2+} reduced both oscillatory translocation and persistent PM localization of PKCβII-EGFP. In TRPC3-deficient cells, although oscillatory movement of PKCβII-EGFP was still observed, the localization of PKCβII-EGFP at the PM was gradually suppressed. The membrane fractionation experiment also showed that both the removal of extracellular Ca^{2+} and the siRNAs against TRPC3 abolished PM accumulation of PKCβII-EGFP after 15 minutes of histamine stimulation (Fig. 4G). These results suggest that TRPC3 channels stabilize PKCβ at the PM also in HeLa cells, raising the possibility that this mechanism is shared by different types of cells.

Sustained PM translocation of PKCβ is important for BCR-induced sustained activation of ERK in DT40 B cells

Previous studies have suggested that PKC is required for the BCR-induced activation of ERK, a MAP kinase (Sakata et al., 1999; Cao et al., 2001; Teixeira et al., 2003; Nishida et al., 2003; Aiba et al., 2004). We examined the roles played by TRPC3 channels in BCR-induced ERK activation via PKC in DT40 B cells (Fig. 5). In WT cells, BCR stimulation maintained the increase in ERK phosphorylation over 45 minutes in the presence of extracellular Ca^{2+}. Strikingly, removal of extracellular Ca^{2+} resulted in transient

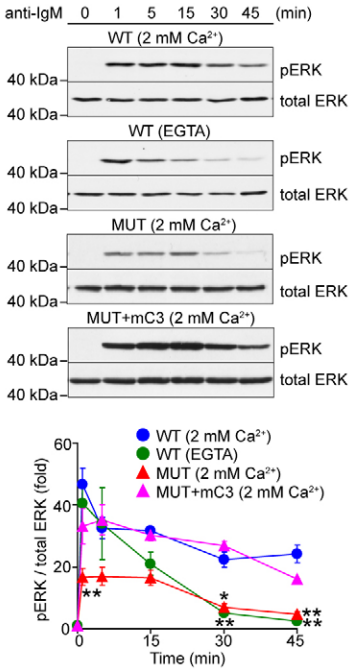

Fig. 5. TRPC3-PKCβ signaling pathway mediates sustained ERK activation. BCR-induced ERK activation in WT and MUT cells. The graph depicts time courses of ERK activation. *P<0.05; **P<0.01, versus WT cells stimulated in the presence of extracellular Ca^{2+}.

ERK activation in WT cells. MUT cells exhibited suppression of ERK activation prominently at the sustained phase and significantly but moderately at the initial phase in the presence of extracellular Ca^{2+}. The sustained ERK activation was restored by the heterologous expression of mC3. Hence, in DT40 B cells, Ca^{2+} influx via TRPC3 channels is required for full ERK activation, in which TRPC3 protein also plays an additional role as a platform for signal transduction at the PM.

Discussion

The results of the present study establish TRPC3 as a DACC that plays an important role in B-cell signaling. TRPC3 channels are responsible for Ca^{2+} influx that induces PM translocation of PLCγ2, and amplification of Ca^{2+} signaling and NFAT activation downstream. Importantly, TRPC3 channels also elicit sustained PM translocation and activation of PKCβ by mediating Ca^{2+} influx and acting as platforms at the PM for PKCβ. Sustained PM translocation of PKCβ has significant impact on downstream ERK activation (Fig. 6).

In MUT DT40 cells expressing an endogenous PM-expression-deficient TRPC3 mutant, suppression of BCR-induced Ca^{2+} influx was attributable to the defect in DAG-activated Ca^{2+} influx (Fig. 1). MUT cells also exhibited impairments in BCR-induced Ca^{2+} oscillations and PLCγ2 accumulation at the PM (Fig. 2), supporting the key role played by DACC TRPC3 in translocation and subsequent secondary activation of PLCγ2 that regulates Ca^{2+} oscillations in the sustained phase of Ca^{2+} signaling in B cells (Nishida et al., 2003). Our previous report demonstrated that the accumulation of PLCγ2 at the PM is completely abolished by the removal of extracellular Ca^{2+} or by treatment with the TRPC3-selective inhibitor Pyr3 (Nishida et al., 2003; Kiyonaka et al., 2009).

Furthermore, overexpression of the PLCγ-interacting mC3(23-73) subfragment significantly suppressed PLCγ2 PM translocation in WT cells, but it failed to restore the defect of PLCγ2 PM translocation in MUT cells (supplementary material Fig. S4C,D). These observations suggest that the accumulation of PLCγ2 at the PM specifically requires both TRPC3-mediated Ca^{2+} influx and the direct interaction between PLCγ2 and PM-localized TRPC3. The specific requirement of TRPC3-mediated Ca^{2+} influx for PM translocation of PLCγ2 is also suggested by the additional finding that a generalized $[Ca^{2+}]_i$ increase by ionomycin and expression of the mC3PD mutant failed to restore BCR-induced PM translocation of PLCγ2 in MUT cells (supplementary material Fig. S4A,B,D).

It has been known that BLNK, also known as SLP65, is the critical scaffolding protein for PLCγ2 in BCR signaling (Fu et al., 1998; Kurosaki et al., 2000). We have not yet studied the exact molecular composition of the signal complex containing TRPC3 and PLCγ2 in DT40 cells to determine whether BLNK is a constituent of this complex. However, considering the fact that both TRPC3 and BLNK positively regulate PLCγ2 activation, it is more likely that TRPC3 and BLNK cooperate in the same complex to amplify BCR signaling than that they compete and antagonize each other. However, an alternative possibility cannot be excluded that BLNK and TRPC3 share the same binding site on PLCγ2 and regulate BCR signaling with different time dependencies.

In different types of cells, sustained Ca^{2+} increase and/or oscillations are required for the activation of NFAT (Gwack et al., 2007). It has been suggested that SOCs form the only major Ca^{2+} influx pathway responsible for NFAT activation in lymphocytes (Feske, 2007). Our previous work in fact demonstrated that disruption of store-operated TRPC1 channels suppresses the frequency of BCR-induced Ca^{2+} oscillations and NFAT activation in DT40 cells (Mori et al., 2002). However, NFAT activity is also reduced in MUT cells (Fig. 2I). Therefore, our study provides evidence for the first time, that Ca^{2+} influx via DAG-activated TRPC3 plays a role in Ca^{2+} oscillations and subsequent NFAT activation in lymphocytes.

With regard to the activation mechanism for cPKC, the coordination of Ca^{2+} and DAG signals is known to determine the kinetics of translocation and activation (Oancea and Meyer, 1998). Recently, Singh et al. suggested that a DAG-activated TRPC6 channel signals the membrane translocation and activation of PKCα, and thereby induces RhoA activation and endothelial contraction (Singh et al., 2007). However, the mechanism underlying PKCα-PM interaction caused by TRPC6-mediated Ca^{2+} entry was not clarified. Our study describes a precise process of cPKC recruitment to the membrane. TRPC3 is capable of providing the sustained Ca^{2+} influx required for sustained PM localization of PKCβ upon BCR stimulation, because DAG is continuously produced by PLCγ2, and TRPC3 activity is in turn sustained. Importantly, to recruit PKCβ to the PM, OAG per se failed but required Ca^{2+} influx via OAG-activated TRPC3 channels (Fig. 3E-G). Furthermore, sustained PM translocation of PKCβ evoked by ionomycin became transient following inhibition of DAG production, and was abolished by disruption of TRPC3 expression at the PM (supplementary material Fig. S5A), suggesting that the sustained PM translocation of PKCβ requires TRPC3-mediated Ca^{2+} influx and persistent production of DAG. Since PKC-mediated phosphorylation has been reported to negatively regulate TRPC3 (Trebak et al., 2003; Venkatachalam et al., 2003; Trebak et al., 2005), the sustained translocation of PKCβ towards PM is the consequence of the TRPC3-mediated Ca^{2+} influx but is unlikely a requisite of

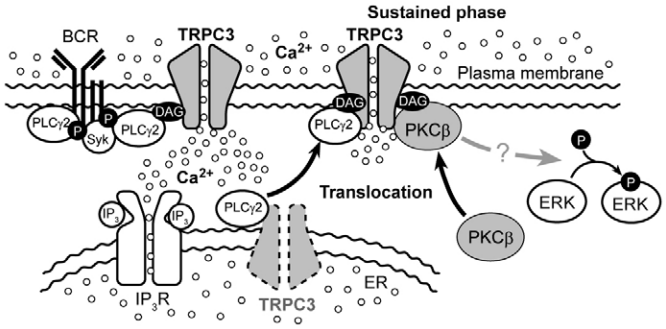

Fig. 6. Proposed model of DAG-activated Ca^{2+} influx mediated by TRPC3 in BCR signaling. BCR stimulation induces PLCγ2 activation via phosphorylation by Syk kinases, and activated PLCγ2 hydrolyses PtdInsP_2 to produce Ins(1,4,5)P_3 (IP_3) and DAG. Ins(1,4,5)P_3 leads to Ca^{2+} release from the ER followed by Ca^{2+} influx via SOCs, whereas DAG induces Ca^{2+} influx via TRPC3. TRPC3-mediated Ca^{2+} influx promotes PLCγ2 translocation from the cytosol to the PM. The targeted PLCγ2 elicits secondary production of Ins(1,4,5)P_3 and DAG to amplify Ca^{2+} signaling via Ins(1,4,5)P_3 receptor-mediated Ca^{2+} release and TRPC3-mediated Ca^{2+} influx, respectively. TRPC3-mediated Ca^{2+} influx is also required for sustained PKCβ membrane translocation and activation, resulting in persistent activation of ERK. TRPC3 protein acts as a platform for PKCβ through direct protein-protein interaction.

TRPC3 activation. Interestingly, in HeLa cells, histamine stimulation evoked oscillatory translocation on top of gradual accumulation of PKCβII-EGFP at the PM, while knockdown of TRPC3 only suppressed the latter (Fig. 4E,F). This suggests that DAG-dependent persistent localization of PKCβII requires TRPC3-mediated Ca^{2+} influx, whereas the oscillatory translocation of PKCβII is induced by repetitive Ca^{2+} spikes in the cytosol. Thus, the persistent localization of cPKCs mediated by DAG-activated Ca^{2+} influx could be a common mechanism shared by many types of cells.

Previous in vitro studies predicted that binding of two Ca^{2+} ions to the C2 domain of PKCβ causes slow and low-affinity membrane interaction and an additional third Ca^{2+} ion subsequently binds to the C2 domain and stabilizes the C2 domain-membrane complex, which allows PKCβ to search for the C1 domain ligand DAG on the membrane (Nalefski and Newton, 2001; Kohout et al., 2002). Notably, it has been proposed that the binding affinity of the third Ca^{2+} ion is too low to promote occupancy except when Ca^{2+} levels reach the millimolar range, or additional groups for Ca^{2+} coordination are provided, as in the presence of phospholipids (Nalefski and Newton, 2001). Since the local Ca^{2+} concentration ($[Ca^{2+}]$) within nanometers of the mouths of Ca^{2+} channels is orders of magnitude larger than bulk cytosolic $[Ca^{2+}]$ (Marsault et al., 1997), TRPC3 may sufficiently augment $[Ca^{2+}]$ to provide the third Ca^{2+} ion to the C2 domain, once PKCβ directly interacts with TRPC3 (Fig. 4A-D). In addition, since TRPC3 also directly interacts with PLCγ2 and regulates PM translocation and activation of PLCγ2, DAG also should be concentrated near TRPC3 and PKCβ. Thus, TRPC3 may increase local concentrations of Ca^{2+} and DAG in organizing the nanodomain that supports sustained PM localization of PKCβ and stabilization of a ternary complex of PKCβ, Ca^{2+} and lipid. Interestingly, it has recently been demonstrated that TRPC3 interacts with a receptor for activated C-kinase-1, which is known to be a scaffolding protein for PKCβ via its N-terminus (Bandyopadhyay et al., 2008). In the *Drosophila* phototransduction system, TRP functions both as a Ca^{2+}-permeable channel and as a

molecular anchor for signalplexes (Li and Montell, 2000). Notably, Leu737-Phe753, the binding region of TRPC3 to PKCβ, is not highly conserved in TRPC6 and TRPC7 (supplementary material Fig. S5B), suggesting a specific function of TRPC3 in anchoring PKCβ at the PM. Thus, TRPC3 stabilizes PKCβ PM localization directly, as a platform, and also indirectly as an amplifier of Ca^{2+} and DAG signals for organizing specific signal complex to achieve specificity and efficiency in BCR-induced signaling.

We can propose a mechanism underlying enhancement of TRPC3 interaction with PKCβ after 15 minutes of BCR stimulation (Fig. 4A). A recent study suggested a control of surface expression of TRPC3 by the interaction between PLCγ1 and TRPC3 (van Rossum et al., 2005). Our data demonstrate that TRPC3-mediated Ca^{2+} influx elicits translocation of PLCγ2 to the PM (Fig. 2G,H; supplementary material Fig. S4) and that the TRP domain is required for proper targeting of TRPC3 proteins to the PM (supplementary material Fig. S1B,C). Therefore, surface expression of TRPC3 is likely to be positively regulated by PLCγ2 membrane translocation in the sustained phase of BCR stimulation, which may consequently augment the interaction between TRPC3 and PKCβ at the PM.

Our study also addresses the mechanisms that link Ca^{2+} influx with BCR-induced ERK activation. In MUT cells, PKCβ translocation and ERK activation was suppressed particularly at later time points after BCR stimulation (Fig. 3A-D, Fig. 5). This is similar to the effect of the cPKC selective inhibitor Gö6976 on ERK activation (Cao et al., 2001), suggesting that PKCβ activity is responsible for the activation of ERK in the sustained phase. Interestingly, it has been reported that TRPC3 regulates brain-derived neurotrophic factor-dependent ERK activation and calcium/cAMP-response element-binding protein phosphorylation in cerebellar granule neurons (Jia et al., 2007). Thus, the regulation of sustained ERK activation by TRPC3 can be shared by various cell types.

Previous studies have correlated differential functional responses of immature and mature B cells with the activation of PKCβ and differences in the duration of ERK activation (King and Monroe, 2000; Koncz et al., 2002). It is possible that the developmentally regulated differential expression of TRPC3 may account for the differences in signaling processes such as the activation of PKCβ and the duration of ERK activation between immature and mature B cells. Alternatively, the production of DAG may be insufficient to activate TRPC3 and PKCβ in immature B cells, since it has been reported that an increase of intracellular Ca^{2+} and hydrolysis of PtdIns(4,5)P_2 are induced in response to BCR cross-linking in mature B cells but an increase of intracellular Ca^{2+} levels is induced in the relative absence of PtdIns(4,5)P_2 hydrolysis in immature B cells (King and Monroe, 2000). These aspects can be addressed using TRPC3 knockout mice, in which B-cell function has not been demonstrated yet (Hartmann et al., 2008; Kim et al., 2009). Interestingly, our preliminary results demonstrated that application of the TRPC3-selective inhibitor Pyr3 (Kiyonaka et al., 2009) suppressed BCR-induced Ca^{2+} responses, sustained PKCβ PM translocation, and ERK activation in murine primary splenic B cells (T.N., unpublished data). Hence, a combination of genetic and pharmacological approaches can reveal the importance of the in vivo DAG-activated TRPC3 channel and its associated mechanism in the context of the developmental maturation of B cells.

Materials and Methods

Cell cultures and cDNA expression

EGFP-fused chicken PKCβII cDNA (Aiba et al., 2004) was first established in the pEGFP-N1 vector (Clontech), and then transferred into pA-puro expression vector (Takata et al., 1994). mC3 cDNA was subcloned into pA-puro vector. DT40 cells were transfected with these constructs by electroporation (550 V, 25 μF) and selected in the presence of 0.5 μg/ml puromycin. WT and PD mutant (in which Leu609, Phe610, Trp611 were changed to alanines) of mC3 (mouse TRPC3) were fused at the C-terminus with mStrawberry and then transferred into pMXΔ (Mori et al., 2002). PKCβ-interacting (Leu726-Phe753) or PLCγ2-interacting (Ser23-Glu73) regions of mC3 were amplified using PCR and fused at the N-terminus with mCherry or mStrawberry, respectively, and cloned into pMXΔ. Cell cultures and cDNA expression in DT40 cells using the vesicular stomatitis virus glycotyped pseudotyped retrovirus were performed as described previously (Mori et al., 2002). An mC3 mutant with deletion of amino acids 667-736 [mC3(Δ667-736)] was constructed using PCR and cloned into pCI-neo (Promega) or pEGFP-N1 to be tagged with EGFP C-terminally. HeLa and HEK293 cells, grown in DMEM supplemented with 10% FBS, were transfected using Superfect (Qiagen) according to the manufacturer's instructions.

Generation of TRPC3-deficient DT40 cells

The chicken genomic *TRPC3* DNA was obtained by PCR using pairs of primers chTRPC3-P1 and chTRPC3-P14, chTRPC3-P5 and chTRPC3-P10, respectively (supplementary material Table S1). The targeting vector was constructed by replacing the genomic sequence, contains the exon corresponding to the sequence distal to the H8 transmembrane region containing TRP domain (EWKFAR) of chicken TRPC3, with a histidinol (*hisD*) or neomycin (*neo*) resistance gene cassette as shown in Fig. 1A (Takata et al., 1994). The upstream 2.1-kb and downstream 4-kb genomic sequences of TRPC3 were used as a targeting vector. The targeting vector transfection and isolation of several clones were performed as described previously (Mori et al., 2002). Clones were further screened by Southern blot analysis of *Xba*I-digested genomic DNA hybridized with a 3′-flanking probe using Gene Images random prime labeling and detection system (GE Healthcare) according to the manufacturer's instructions.

Measurement of changes in $[Ca^{2+}]_i$

Measurement of changes in $[Ca^{2+}]_i$ was performed, as we previously described (Mori et al., 2002). Images of the fura-2 fluorescence of the cells were recorded in a physiological salt solution (PSS; in mM): 150 NaCl, 8 KCl, 2 $CaCl_2$, 1 $MgCl_2$, 5 Hepes, 5.6 glucose (pH 7.4 adjusted with NaOH), and analyzed with a video image analysis system (Aqua Cosmos; Hamamatsu Photonics). The Ca^{2+}-free solution contained 0.5 mM EGTA but no added $CaCl_2$.

Immunofluorescence staining

DT40 cells were fixed with 4% paraformaldehyde for 5 minutes, immobilized on slides using cytospin centrifugation, and permeabilized with 0.2% Triton X-100 for 5 minutes. After blocking with 5% BSA, cells were incubated with anti-TRPC3 antibody for 2 hours (Nishida et al., 2003). The primary antibodies were detected using anti-rabbit secondary antibodies labeled with Alexa Fluor 488 (Invitrogen).

Electrophysiology

Measurements of OAG-activated currents and I_{CRAC} were carried out as described previously (Inoue et al., 2001; Mori et al., 2002). For measurement of OAG-activated current, DT40 cells were allowed to settle in the perfusion chamber for 5 minutes in the external solution (in mM): 140 NaCl, 5 KCl, 1.5 $MgCl_2$, 1 $CaCl_2$, 10 Hepes, 10 glucose (pH 7.4 adjusted with Tris base). The pipette solution contained (in mM): 120 CsOH, 120 aspartate, 20 CsCl, 5 creatine, 2 $MgSO_4$, 5 EGTA, 2 ATP, 5 Hepes (pH 7.2 adjusted with Tris base). For measurements of I_{CRAC}, DT40 cells were suspended in standard external, modified Ringer's solution (in mM): 135 NaCl, 2.8 KCl, 10 CsCl, 2 $MgCl_2$, 10 $CaCl_2$, 10 glucose, 5 Hepes (pH 7.4 adjusted with NaOH). The standard pipette solution contained (in mM): 132 CsOH, 132 glutamate, 6 NaCl, 1 $MgCl_2$, 10 EGTA, 2 MgATP, 0.2 GTP, 0.01 Ins(1,4,5)P_3, 5 Hepes (pH 7.2 adjusted with CsOH).

Confocal microscopy and image analysis

Fluorescent protein-expressing DT40 or HeLa cells were plated onto poly-L-lysine-coated glass coverslips. Fluorescence images were acquired with a confocal laser-scanning microscope (FV500; Olympus) using the 488-nm line of an argon laser for excitation and a 505-nm to 525-nm band-pass filter for emission (EYFP or EGFP), or the 543-nm line of a HeNe laser for excitation and a 560-nm long-pass filter for emission (mStrawberry or mCherry). The specimens were viewed at high magnification using plan oil objectives (60×, 1.40 NA; Olympus). DT40 cells were stimulated with 1 μg/ml anti-IgM or 0.3 μM OAG. HeLa cells were stimulated with 100 μM histamine. To obtain a measure of the membrane translocation of PLCγ2 and PKCβII, regions of interest (ROI) were defined over the outer border (typical thickness of regions, 0.5 μm; Fig. 2G). Fluorescence intensities over the expected localization of the PM (F_{PM}) were divided by the fluorescence intensities over the whole cell (F_{total}) and expressed as percentages of total fluorescence. For experiments shown in Fig. 4E, confocal images were recorded for 15 minutes at 10-second intervals. Non-overlapping ROI of identical size were placed on the PM and cytosol of each PKCβII-EGFP-positive HeLa cell (Fig. 4E). The average fluorescence intensity for each ROI were measured during the recording, and the ratio ($F_{PM}/F_{cytosol}$) was calculated. These values were then plotted as a function of time and normalized to the fluorescence intensities recorded at time 0. To quantify changes of fluorescence

increase in the PM after 15 minutes of histamine stimulation in HeLa cells (shown in Fig. 4E), the fluorescence intensities of the PM were averaged and normalized according to the following equation: $\Delta R=(R-R_0)/R_0$, where R is the ratio of fluorescence intensity of the PM to that of the whole cell at 15 minutes after histamine stimulation, and R_0 is the ratio at time 0.

NFAT reporter assay

NFAT activity was quantified with 1420 ARVOsx (Wallac) using NFAT luciferase genes (Stratagene) and the Dual-Luciferase™ assay system (Promega) as described previously (Sugawara et al., 1997).

Separation of membrane and cytosolic fractions

DT40 or HeLa cells were stimulated with 10 μg/ml anti-IgM or 100 μM histamine in serum-free PSS, respectively. Membrane fractionation was performed as described previously (Krotova et al., 2003). Samples were resolved by SDS-PAGE and subjected to immunoblotting with anti-PKCβ monoclonal antibody (BD Transduction Laboratories). The bands were scanned and the density of each band was determined using ImageJ software.

Immunoprecipitation

DT40 cells were stimulated with 10 μg/ml anti-IgM, and lysed in NP-40 lysis buffer (137 mM NaCl, 20 mM Tris-HCl, pH 8.0, 10% glycerol, 1% NP-40, 2 mM EDTA, 1 mM PMSF, 20 μg/ml leupeptin, 0.1 μg/ml aprotinin and 5 mM sodium orthovanadate). HEK293 cells expressing PLCγ2-EGFP with mC3 or mC3(Δ667-736) were lysed as described previously (Kiyonaka et al., 2009). The cell lysate was further subjected to immunoprecipitation as described previously (Nishida et al., 2003) using anti-PKCα antibody (BD Transduction Laboratories) which cross-reacts with PKCβ (Fig. 4A) or anti-TRPC3 (supplementary material Fig. S4A). The immunocomplexes were characterized by immunoblotting with anti-TRPC3 antibody (Fig. 4A) or with anti-GFP antibody (supplementary material Fig. S4A).

GST pull-down assay

cDNAs for mC3 fragments and the GST were subcloned into the pET23 vector (Novagen). Purification of GST fusion proteins and pull-down assays were performed as described previously (Kiyonaka et al., 2007). DT40 cells were lysed in NP-40 lysis buffer. Purified human PKCβII was obtained from Sigma. The samples were subjected to immunoblotting using anti-PKCβ antibody.

RNA interference

HeLa cells were transfected 72 hours prior to confocal analysis with siRNA duplex using Oligofectamine (Invitrogen) according to manufacturer's instructions. TRPC3 was targeted using two siRNA oligonucleotides directed against the sequences: 5′-UCUUGAGUUAGACUGAGUGAAGAGG-3′ and 5′-AUAACGUGUUGGCUGAUUGAGAAUG-3′. The sequence of randomized siRNA was: 5′-CAUAACUGACUAACCGCACUCUUAU-3′.

Expression analysis

The PCR protocol used for the expression analysis was described previously (Inoue et al., 2001). The PCR primers used are listed in supplementary material Table S1.

Analysis of ERK activity

DT40 cells were stimulated with 10 μg/ml anti-IgM in serum-free PSS and then lysed as described previously (Nishida et al., 2003).

Flow cytometric analysis

Cell surface expression of BCR on WT and MUT cells was analyzed with Epics Altra (Beckman Coulter) using a FITC-conjugated anti-chicken IgM antibody (Bethyl) as previously described (Aiba et al., 2004).

Statistical analysis

All data are expressed as means ± s.e.m. The data represent at least three independent experiments for each condition. Statistical significance was evaluated using the Student's *t*-test for comparisons between two mean values. Multiple comparisons between more than three groups were carried out using an ANOVA followed by Tukey-Kramer test.

We thank Y. Aiba and S. Yamamoto for much technical advice and helpful discussions, and R. Y. Tsien for mCherry and mStrawberry. This study was supported by research grants from Ministry of Education, Culture, Sports, Science and Technology of Japan and the Japan Society for the Promotion of Sciences, and in part by the Intramural Program of the NIH, National Institute of Environmental Health Sciences. Deposited in PMC for release after 12 months.

Supplementary material available online at
http://jcs.biologists.org/cgi/content/full/123/6/927/DC1

References

Aiba, Y., Oh-hora, M., Kiyonaka, S., Kimura, Y., Hijikata, A., Mori, Y. and Kurosaki, T. (2004). Activation of RasGRP3 by phosphorylation of Thr-133 is required for B cell receptor-mediated Ras activation. *Proc. Natl. Acad. Sci. USA* **101**, 16612-16617.

Bandyopadhyay, B. C., Ong, H. L., Lockwich, T. P., Liu, X., Paria, B. C., Singh, B. B. and Ambudkar, I. S. (2008). TRPC3 controls agonist-stimulated intracellular Ca^{2+} release by mediating the interaction between inositol 1,4,5-trisphosphate receptor and RACK1. *J. Biol. Chem.* **283**, 32821-32830.

Berridge, M. J. (1993). Inositol trisphosphate and calcium signalling. *Nature* **361**, 315-325.

Bird, G. S., Aziz, O., Lievremont, J. P., Wedel, B. J., Trebak, M., Vazquez, G. and Putney, J. W., Jr (2004). Mechanisms of phospholipase C-regulated calcium entry. *Curr. Mol. Med.* **4**, 291-301.

Cao, M. Y., Shinjo, F., Heinrichs, S., Soh, J. W., Jongstra-Bilen, J. and Jongstra, J. (2001). Inhibition of anti-IgM-induced translocation of protein kinase C βI inhibits ERK2 activation and increases apoptosis. *J. Biol. Chem.* **276**, 24506-24510.

Fasolato, C., Innocenti, B. and Pozzan, T. (1994). Receptor-activated Ca^{2+} influx: how many mechanisms for how many channels? *Trends Pharmacol. Sci.* **15**, 77-83.

Feske, S. (2007). Calcium signalling in lymphocyte activation and disease. *Nat. Rev. Immunol.* **7**, 690-702.

Feske, S., Giltnane, J., Dolmetsch, R., Staudt, L. M. and Rao, A. (2001). Gene regulation mediated by calcium signals in T lymphocytes. *Nat. Immunol.* **2**, 316-324.

Fu, C., Turck, C. W., Kurosaki, T. and Chan, A. C. (1998). BLNK: a central linker protein in B cell activation. *Immunity* **9**, 93-103.

Gallo, E. M., Canté-Barrett, K. and Crabtree, G. R. (2006). Lymphocyte calcium signaling from membrane to nucleus. *Nat. Immunol.* **7**, 25-32.

Gwack, Y., Feske, S., Srikanth, S., Hogan, P. G. and Rao, A. (2007). Signalling to transcription: store-operated Ca^{2+} entry and NFAT activation in lymphocytes. *Cell Calcium* **42**, 145-156.

Hartmann, J., Dragicevic, E., Adelsberger, H., Henning, H. A., Sumser, M., Abramowitz, J., Blum, R., Dietrich, A., Freichel, M., Flockerzi, V. et al. (2008). TRPC3 channels are required for synaptic transmission and motor coordination. *Neuron* **59**, 392-398.

Hofmann, T., Obukhov, A. G., Schaefer, M., Harteneck, C., Gudermann, T. and Schultz, G. (1999). Direct activation of human TRPC6 and TRPC3 channels by diacylglycerol. *Nature* **397**, 259-263.

Hofmann, T., Schaefer, M., Schultz, G. and Gudermann, T. (2000). Transient receptor potential channels as molecular substrates of receptor-mediated cation entry. *J. Mol. Med.* **78**, 14-25.

Inoue, R., Okada, T., Onoue, H., Hara, Y., Shimizu, S., Naitoh, S., Ito, Y. and Mori, Y. (2001). The transient receptor potential protein homologue TRP6 is the essential component of vascular α_1-adrenoceptor-activated Ca^{2+}-permeable cation channel. *Circ. Res.* **88**, 325-332.

Jia, Y., Zhou, J., Tai, Y. and Wang, Y. (2007). TRPC channels promote cerebellar granule neuron survival. *Nat. Neurosci.* **10**, 559-567.

Kim, M. S., Hong, J. H., Li, Q., Shin, D. M., Abramowitz, J., Birnbaumer, L. and Muallem, S. (2009). Deletion of TRPC3 in mice reduces store-operated Ca^{2+} influx and the severity of acute pancreatitis. *Gastroenterology* **137**, 1509-1517.

King, L. B. and Monroe, J. G. (2000). Immunobiology of the immature B cell: plasticity in the B-cell antigen receptor-induced response fine tunes negative selection. *Immunol. Rev.* **176**, 86-104.

Kiyonaka, S., Wakamori, M., Miki, T., Uriu, Y., Nonaka, M., Bito, H., Beedle, A. M., Mori, E., Hara, Y., De Waard, M. et al. (2007). RIM1 confers sustained activity and neurotransmitter vesicle anchoring to presynaptic Ca^{2+} channels. *Nat. Neurosci.* **10**, 691-701.

Kiyonaka, S., Kato, K., Nishida, M., Mio, K., Numaga, T., Sawaguchi, Y., Yoshida, T., Wakamori, M., Mori, E., Numata, T. et al. (2009). Selective and direct inhibition of TRPC3 channels underlies biological activities of a pyrazole compound. *Proc. Natl. Acad. Sci. USA* **106**, 5400-5405.

Kohout, S. C., Corbalán-García, S., Torrecillas, A., Goméz-Fernandéz, J. C. and Falke, J. J. (2002). C2 domains of protein kinase C isoforms α, β, and γ: activation parameters and calcium stoichiometries of the membrane-bound state. *Biochemistry* **41**, 11411-11424.

Koncz, G., Bodor, C., Kövesdi, D., Gáti, R. and Sármay, G. (2002). BCR mediated signal transduction in immature and mature B cells. *Immunol. Lett.* **82**, 41-49.

Krotova, K. Y., Zharikov, S. I. and Block, E. R. (2003). Classical isoforms of PKC as regulators of CAT-1 transporter activity in pulmonary artery endothelial cells. *Am. J. Physiol. Lung. Cell Mol. Physiol.* **284**, L1037-L1044.

Kurosaki, T. and Tsukada, S. (2000). BLNK: connecting Syk and Btk to calcium signals. *Immunity* **12**, 1-5.

Le Deist, F., Hivroz, C., Partiseti, M., Thomas, C., Buc, H. A., Oleastro, M., Belohradsky, B., Choquet, D. and Fischer, A. (1995). A primary T-cell immunodeficiency associated with defective transmembrane calcium influx. *Blood* **85**, 1053-1062.

Leitges, M., Schmedt, C., Guinamard, R., Davoust, J., Schaal, S., Stabel, S. and Tarakhovsky, A. (1996). Immunodeficiency in protein kinase cβ-deficient mice. *Science* **273**, 788-791.

Lewis, R. S. (2001). Calcium signaling mechanisms in T lymphocytes. *Annu. Rev. Immunol.* **19**, 497-521.

Li, H. S. and Montell, C. (2000). TRP and the PDZ protein, INAD, form the core complex required for retention of the signalplex in *Drosophila* photoreceptor cells. *J. Cell Biol.* **150**, 1411-1422.

Lintschinger, B., Balzer-Geldsetzer, M., Baskaran, T., Graier, W. F., Romanin, C., Zhu, M. X. and Groschner, K. (2000). Coassembly of Trp1 and Trp3 proteins generates diacylglycerol- and Ca^{2+}-sensitive cation channels. *J. Biol. Chem.* **275**, 27799-27805.

Liu, Q. H., Liu, X., Wen, Z., Hondowicz, B., King, L., Monroe, J. and Freedman, B. D. (2005). Distinct calcium channels regulate responses of primary B lymphocytes to B cell receptor engagement and mechanical stimuli. *J. Immunol.* **174**, 68-79.

Liu, W. S. and Heckman, C. A. (1998). The sevenfold way of PKC regulation. *Cell Signal.* **10**, 529-542.

Lucas, P., Ukhanov, K., Leinders-Zufall, T. and Zufall, F. (2003). A diacylglycerol-gated cation channel in vomeronasal neuron dendrites is impaired in *TRPC2* mutant mice: mechanism of pheromone transduction. *Neuron* **40**, 551-561.

Maasch, C., Wagner, S., Lindschau, C., Alexander, G., Buchner, K., Gollasch, M., Luft, F. C. and Haller, H. (2000). Protein kinase cα targeting is regulated by temporal and spatial changes in intracellular free calcium concentration $[Ca^{2+}]_i$. *FASEB J.* **14**, 1653-1663.

Marsault, R., Murgia, M., Pozzan, T. and Rizzuto, R. (1997). Domains of high Ca^{2+} beneath the plasma membrane of living A7r5 cells. *EMBO J.* **16**, 1575-1581.

Mischak, H., Kolch, W., Goodnight, J., Davidson, W. F., Rapp, U., Rose-John, S. and Mushinski, J. F. (1991). Expression of protein kinase C genes in hemopoietic cells is cell-type- and B cell-differentiation stage specific. *J. Immunol.* **147**, 3981-3987.

Mogami, H., Zhang, H., Suzuki, Y., Urano, T., Saito, N., Kojima, I. and Petersen, O. H. (2003). Decoding of short-lived Ca^{2+} influx signals into long term substrate phosphorylation through activation of two distinct classes of protein kinase C. *J. Biol. Chem.* **278**, 9896-9904.

Montell, C. and Rubin, G. M. (1989). Molecular characterization of the Drosophila *trp* locus: a putative integral membrane protein required for phototransduction. *Neuron* **2**, 1313-1323.

Mori, Y., Wakamori, M., Miyakawa, T., Hermosura, M., Hara, Y., Nishida, M., Hirose, K., Mizushima, A., Kurosaki, M., Mori, E. et al. (2002). Transient receptor potential 1 regulates capacitative Ca^{2+} entry and Ca^{2+} release from endoplasmic reticulum in B lymphocytes. *J. Exp. Med.* **195**, 673-681.

Nalefski, E. A. and Newton, A. C. (2001). Membrane binding kinetics of protein kinase C βII mediated by the C2 domain. *Biochemistry* **40**, 13216-13229.

Nishida, M., Sugimoto, K., Hara, Y., Mori, E., Morii, T., Kurosaki, T. and Mori, Y. (2003). Amplification of receptor signalling by Ca^{2+} entry-mediated translocation and activation of PLCγ2 in B lymphocytes. *EMBO J.* **22**, 4677-4688.

Nishida, M., Hara, Y., Yoshida, T., Inoue, R. and Mori, Y. (2006). TRP channels: molecular diversity and physiological function. *Microcirculation* **13**, 535-550.

Nishizuka, Y. (1995). Protein kinase C and lipid signaling for sustained cellular responses. *FASEB J.* **9**, 484-496.

Oancea, E. and Meyer, T. (1998). Protein kinase C as a molecular machine for decoding calcium and diacylglycerol signals. *Cell* **95**, 307-318.

Okada, T., Inoue, R., Yamazaki, K., Maeda, A., Kurosaki, T., Yamakuni, T., Tanaka, I., Shimizu, S., Ikenaka, K., Imoto, K. et al. (1999). Molecular and functional characterization of a novel mouse transient receptor potential protein homologue TRP7. Ca^{2+}-permeable cation channel that is constitutively activated and enhanced by stimulation of G protein-coupled receptor. *J. Biol. Chem.* **274**, 27359-27370.

Onohara, N., Nishida, M., Inoue, R., Kobayashi, H., Sumimoto, H., Sato, Y., Mori, Y., Nagao, T. and Kurose, H. (2006). TRPC3 and TRPC6 are essential for angiotensin II-induced cardiac hypertrophy. *EMBO J.* **25**, 5305-5316.

Parekh, A. B. and Putney, J. W., Jr (2005). Store-operated calcium channels. *Physiol. Rev.* **85**, 757-810.

Partiseti, M., Le Deist, F., Hivroz, C., Fischer, A., Korn, H. and Choquet, D. (1994). The calcium current activated by T cell receptor and store depletion in human lymphocytes is absent in a primary immunodeficiency. *J. Biol. Chem.* **269**, 32327-32335.

Peng, S. L., Gerth, A. J., Ranger, A. M. and Glimcher, L. H. (2001). NFATc1 and NFATc2 together control both T and B cell activation and differentiation. *Immunity* **14**, 13-20.

Pinton, P., Tsuboi, T., Ainscow, E. K., Pozzan, T., Rizzuto, R. and Rutter, G. A. (2002). Dynamics of glucose-induced membrane recruitment of protein kinase C βII in living pancreatic islet β-cells. *J. Biol. Chem.* **277**, 37702-37710.

Putney, J. W., Jr (1990). Capacitative calcium entry revisited. *Cell Calcium* **11**, 611-624.

Rao, A., Luo, C. and Hogan, P. G. (1997). Transcription factors of the NFAT family: regulation and function. *Annu. Rev. Immunol.* **15**, 707-747.

Reither, G., Schaefer, M. and Lipp, P. (2006). PKCα: a versatile key for decoding the cellular calcium toolkit. *J. Cell Biol.* **174**, 521-533.

Sakata, N., Kawasome, H., Terada, N., Gerwins, P., Johnson, G. L. and Gelfand, E. W. (1999). Differential activation and regulation of mitogen-activated protein kinases through the antigen receptor and CD40 in human B cells. *Eur. J. Immunol.* **29**, 2999-3008.

Singh, I., Knezevic, N., Ahmmed, G. U., Kini, V., Malik, A. B. and Mehta, D. (2007). $Gα_q$-TRPC6-mediated Ca^{2+} entry induces RhoA activation and resultant endothelial cell shape change in response to thrombin. *J. Biol. Chem.* **282**, 7833-7843.

Sugawara, H., Kurosaki, M., Takata, M. and Kurosaki, T. (1997). Genetic evidence for involvement of type 1, type 2 and type 3 inositol 1,4,5-trisphosphate receptors in signal transduction through the B-cell antigen receptor. *EMBO J.* **16**, 3078-3088.

Takata, M., Sabe, H., Hata, A., Inazu, T., Homma, Y., Nukada, T., Yamamura, H. and Kurosaki, T. (1994). Tyrosine kinases Lyn and Syk regulate B cell receptor-coupled Ca^{2+} mobilization through distinct pathways. *EMBO J.* **13**, 1341-1349.

Teixeira, C., Stang, S. L., Zheng, Y., Beswick, N. S. and Stone, J. C. (2003). Integration of DAG signaling systems mediated by PKC-dependent phosphorylation of RasGRP3. *Blood* **102**, 1414-1420.

Thebault, S., Flourakis, M., Vanoverberghe, K., Vandermoere, F., Roudbaraki, M., Lehen'kyi, V., Slomianny, C., Beck, B., Mariot, P., Bonnal, J. L. et al. (2006). Differential role of transient receptor potential channels in Ca^{2+} entry and proliferation of prostate cancer epithelial cells. *Cancer Res.* **66**, 2038-2047.

Trebak, M., Bird, G. St J., McKay, R. R., Birnbaumer, L. and Putney, J. W., Jr (2003). Signaling mechanism for receptor-activated canonical transient receptor potential 3 (TRPC3) channels. *J. Biol. Chem.* **278**, 16244-16252.

Trebak, M., Hempel, N., Wedel, B. J., Smyth, J. T., Bird, G. S. and Putney, J. W., Jr (2005). Negative regulation of TRPC3 channels by protein kinase C-mediated phosphorylation of serine 712. *Mol. Pharmacol.* **67**, 558-563.

van Rossum, D. B., Patterson, R. L., Sharma, S., Barrow, R. K., Kornberg, M., Gill, D. L. and Snyder, S. H. (2005). Phospholipase Cγ1 controls surface expression of TRPC3 through an intermolecular PH domain. *Nature* **434**, 99-104.

Venkatachalam, K., Zheng, F. and Gill, D. L. (2003). Regulation of canonical transient receptor potential (TRPC) channel function by diacylglycerol and protein kinase C. *J. Biol. Chem.* **278**, 29031-29040.

Violin, J. D., Zhang, J., Tsien, R. Y. and Newton, A. C. (2003). A genetically encoded fluorescent reporter reveals oscillatory phosphorylation by protein kinase C. *J. Cell Biol.* **161**, 899-909.

Welsh, D. G., Morielli, A. D., Nelson, M. T. and Brayden, J. E. (2002). Transient receptor potential channels regulate myogenic tone of resistance arteries. *Circ. Res.* **90**, 248-250.